AADE-17-NTCE-026

Theoretical Modeling of Positive Displacement Motor Performance

Tan C. Nguyen and Khiem D. Bui, New Mexico Tech;
Eissa Al-Safran, Kuwait University; Arild Saasen, University of Stavanger

Abstract

Positive Displacement Motor (PDM) has been used extensively in directional and horizontal drilling operations. There are no reliable analytical models to predict the performance of PDMs. Based on motor geometry, each PDM has its own unique performance that is experimentally obtained by manufacturers using water as a testing fluid. These experiments are not only costly and time-consuming, but also with conditions that do not represent the actual down-hole conditions.

The key to improve the prediction of motor performance is to, accurately; determine the flowing cross-sectional area of PDM. This paper uses Nguyen et al. (2014) model for calculating the flow area of a multi-lobe progressing cavity pump, in addition to two developed analytical models for predicting the actual performance of a multi-lobe PDM. A sensitivity analysis was performed to optimize motor geometry to maximize motor torque. The developed models were validated using experimental data from a single 1:2-lobe and multi 2:3-lobe PDMs. The results revealed that when the stator lobe number is greater than five, torque is maximized if the dimensionless motor geometry is zero. The flowing cross-sectional area is reduced when the stator lobe number is higher than four. However, the flow rate is always higher when the stator lobe number is increased. The results also showed that it is not recommended designing a PDM which has the stator lobe greater than twelve. Furthermore, model validation showed that the proposed models predict the actual multi-lobe PDM performance with average percent error of less than 6% when differential pressure across the motor is 300 psi or less. The results of the present study are not only important for manufacturers to optimize PDM design, but also for operators to improve the performance and efficiency of PDMs.

Introduction

There are two types of downhole mud motors, namely Positive Displacement Motor (PDM), and Downhole Turbine Motor (DTM). The PDM has been te most common motor in the United States with about 99% of the total footage drilled in the United States (Li et al., 1998). A PDM is a hydraulically driven down-hole motor, which drives drill bit without rotating drill-string and uses the Moineau principle (Moineau, 1932). Moineau design composed of two helical gears, one inside the other, where the rotor rotates around its longitudinal axis in parallel with the stator axis. The internal gear always has one extra lobe than the external one. The rotor is designed so that all the lobes of the rotor are constantly in contact with the stator. As the drilling fluid is forced into the motor, fluid hydraulic power drives the rotor in an eccentric rotation, which is then transferred into concentric rotation through a universal joint assembly, which is transferred to drill bit.

A basic PDM is composed of the following parts: sealed bearing assembly, adjustable housing and drive shaft, power section, and dump sub (Courgar Drilling Solution Handbook, 2012). The sealed bearing assembly carries all radial and thrust loading, where the sealing is used to deliver maximum flow to drill-bit. The adjustable housing connects the stator to the bearing assembly housings, and houses the drive shaft assembly. The power section converts hydraulic power from drilling fluid into torque required to rotate the rotor. Dump sub is a by-pass valve installed above the motor, which allows drilling fluid to fill the drill-string during tripping in and to drain drill-string when tripping out. PDMs are economic and technically appropriate as directional drilling tool. They have been effective in drilling rate, side tracking, hole straightening, and horizontal drilling with the use of adjustable or fixed housing (Roberts and Mohr, 1972). In addition, when an angle is selected in the adjustable or fixed housing, the bit face is oriented to initiate a build or a drop angle in wellbore. As drill bit reaches the kick-off depth, motor is tripped out to re-adjust bend angle, then motor is tripped in to resume build or drop angle drilling.

Mud motor should be selected properly to match bit torque requirements and flow rates to reach and efficient hole-cleaning, and maximum pump pressure. Furthermore, it is crucial to monitor standpipe pressure during downhole mud motor operation. Initially, as motor starts in off-bottom position, standpipe pressure increases until the motor starts rotating, which depends on motor size and geometry, drill-pipe size, drill-collars, and other tools installed in drill-string. If drill-bit is close to the bottom of the hole and the motor is installed near drill bit, standpipe pressure in Pa is given as,

$$P_{standpipe} = P_{wf} - \rho_m g TVD + \Delta P_f^{dp} + \Delta P_{motor} \qquad (1)$$

where P_{wf} is flowing bottom-hole pressure while drilling (Pa), ρ_m is drilling fluid density (kg/m^3), TVD is well true vertical depth (m), ΔP_f^{dp} is frictional pressure drop in drill-string (Pa), and ΔP_{motor} is motor pressure drop (Pa). Note that regions, e.g. key-seats may cause higher standpipe pressure to initiate motor rotation if the motor is disoriented.

As the motor rotates and the well is being drilled, the stand-pipe pressure must be sufficient to overcome the frictional pressure loss inside the drill-string and in the annuli, the pressure drop across the drill-bit, and the pressure drop inside the motor. The pressure drop inside the motor has two components: the pressure drop to initiate the rotation and the pressure drop to overcome the friction between the bit and the formation rock, given the Weight On Bit (WOB). The equation to calculate the stand-pipe pressure as the well is being drilled is presented as follows:

$$P_{standpipe} = \Delta P_f^{dp} + \Delta P_f^{ann} + \Delta P_b + \Delta P_{motor} \qquad (2)$$

where ΔP_f^{ann} and ΔP_b are the frictional pressure loss in the annulus and the pressure drop at the drill-bit. As drilling commences, the WOB may be increased to reach the desired Rate of Penetration (ROP), maximum torque or maximum motor differential pressure. However, the stand-pipe pressure should not exceed the value that causes the motor differential pressure to be higher than the maximum differential pressure for a given motor size. As cuttings are generated into the drilling fluid, some hydraulic power will be lost to lift these cuttings and hence the stand-pipe pressure predicted by Eq. (2) can vary slightly. If the applied WOB is too high, the motor stall may occur and the bit stops rotating. If the motor stall happens, the stand-pipe pressure increases rapidly; the surface measured torque will be very high causing a possible damage to motor components. Keep pumping drilling fluid through a stalled motor may cause wear to the stator elastomer and damage to the sealed bearing.

Makohl and Jurgens (1986) proposed a comprehensive PDM drilling program, which extends tool life, increases motor reliability, optimizes motor efficiency, improves PDM performance for different drilling operations, and increases motor power. By selecting different materials stator elastomer, they claimed that the PDMs could be operated under down-hole conditions for more than 100 hours without maintenance. Their program is based on experimental study of the effect of lobe number on motor efficiency, concluding that 1:2-lobe motor operated has best efficiency at medium to high-speed ranges. When the number of lobes increased, the maximum efficiency is reduced 50% as in the case of 9:10-lobe motor, recommending low speed operating to achieve high efficiency. The authors also studied the impact of different motor geometries on motor power and efficiency, and generated performance charts based on the experimental data, that is limited in application.

Samuel presented a mathematical model for the performance of positive PDMs for incompressible fluids (Samuel et al., 1997 and 2003). Equations were introduced for calculating the cross-sectional flowing area, volumetric flow rate, torque, power and slippage in the multi-lobe motor. The cross-sectional flowing area in Samuel's paper was defined as the difference in cross-sectional flowing area between the two circles: motor housing (stator) and shaft (rotor). This definition is very conservative because it does not take into account the actual geometry of the PDM. In addition, all the flow rates, torque, powers formulas are directly related to the cross-sectional flowing area equation and hence all of these formulas have a systematic error. The cross section of each lobe of the rotor or stator of an actual PDM has the shape of a semicircle. The semicircle diameter and the motor eccentricity must be taken into account to accurately calculate the cross-sectional flowing area of the PDM. How to consider the semicircle diameter and the motor eccentricity into the model will be presented in detail in the model development section of the current paper.

Li et al. (1998) presented the PDM's performance by using dimensionless groups. In general, the performance of a PDM is a function of the torque, flow-rate, rotational speed, pressure drop, motor's geometries, and fluid properties. They used the Buckingham theorem to develop eight different dimensionless groups. After rearranging, the eight dimensionless groups were simplified and reduced down to three groups. The authors claimed that with these three dimensionless groups, the performance of PDMs can be described by both geometric parameters of the motor and the rheological properties of the circulation fluid.

An analytical model to predict the performance of a multi-lobe progressive cavity pump was developed by Nguyen et al. (2014), using vector analysis and hypocycloid theory to develop flowing cross-sectional area for multi-lobe progressive cavity pumps. Model validation study against experimental data showed model prediction less than 4% average error for pump differential pressures less than 200 psi and fluid viscosities of 200 cp or higher. This study applies this analytical model to predict the actual performance of PDMs under field conditions. The model is validated against 1:2-lobe and 2:3-lobe PDMs experimental data. A thorough analysis is also carried out to optimize the design of a PDM.

Theoretical Modeling

The original cross-section of a Moineau motor has a hypocycloid shape. **Fig. 1** show a 3-lobe and a 4-lobe hypocycloid, which are generated by tracing a fixed point on a generator circle with a diameter of D_g within a base circle of a diameter D_b. The ratio between the diameter of base circle to generator circle, D_b/D_g, is same as number of lobes, K. However, the actual cross-sectional shape of a PDM is not as the original hypocycloid. To create the modified hypocycloid, Nguyen et al. (2014) proposed that a semicircle with a diameter d is added at each cusp of the original hypocycloid with each point moving with a distance of d/2, following the

direction of unit normal vector at this point. A modified 4-lobe and 3-lobe hypocycloid is shown in **Fig. 2**. According to Nguyen et al. (2014), the total cross-sectional flowing area of a K-lobe modified hypocycloid is given as,

$$A_K = 2\pi e^2 - \pi\left(\frac{d^2}{8} + e^2\right)(K^2 - 3K) - \frac{de}{2}(K^2 - 8K + 7) \quad (3)$$

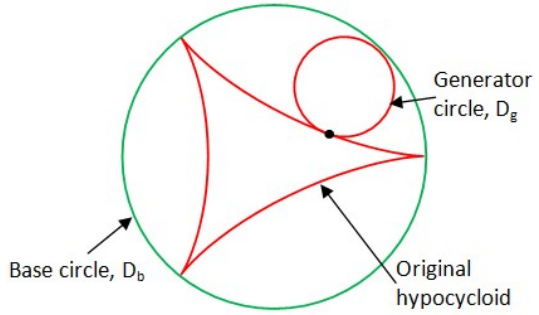

a: 3-lobe hypocycloid ; K = 3 ; $D_b = 3D_g$.

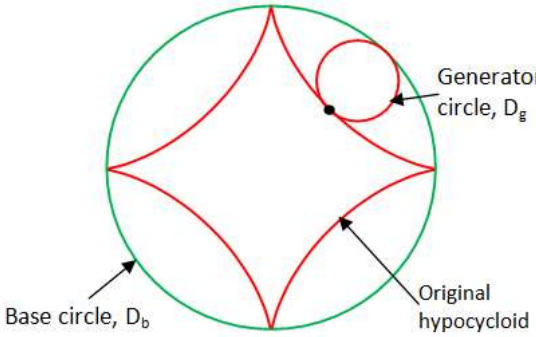

b: 4-lobe hypocycloid ; K = 4 ; $D_b = 4D_g$.

Figure 1: Cross-section of Moineau pump

In general, an actual PDM will consist of a K-lobe modified hypocycloid (K-lobe stator) and (K-1)-lobe modified hypocycloid, thus the flowing cross sectional area of PDM is given as,

$$A_F = A_K - A_{K-1} = 2\pi e^2(K - 2) + 4de \quad (4)$$

For a single lobe 1:2 PDM, the cross-sectional flowing area is:

$$A_F = 4de \quad (5)$$

where d is the diameter of the semicircle at each cusp of the original hypocycloid, e is the motor eccentricity defined as the difference between stator and rotor radii. Therefore, eccentricity is the radius of the generator circle, r_g, as shown in Eq. 6.

$$e = r_s - r_r = Kr_g - (K - 1)r_g = r_g \quad (6)$$

where r_s, r_r, and r_g are the radii of stator, rotor, and generator circle, respectively. Note that the relationship between the diameters of base, D_b, and generator, D_g, circles for one hypocycloid is expressed as,

$$D_b = KD_g \quad or \quad r_b = Kr_g \quad (7)$$

Combining Eq. (6) and Eq. (7) gives,

$$e = \frac{r_b}{K} = \frac{D_b}{2K} \quad (8)$$

For a K-lobe PDM, the eccentricity can be calculated as,

$$e = \frac{D_{bs}}{2K} = \frac{D_{br}}{2(K - 1)} \quad (9)$$

where D_{bs} and D_{br} are the diameters of stator base and rotor base circles, respectively, as shown in **Fig. 2**. The diameters of the stator and rotor of a PDM are given as,

$$D_s = D_{bs} + d = 2eK + \quad (10)$$

$$D_r = D_{br} + d = 2e(K - 1) + d \quad (11)$$

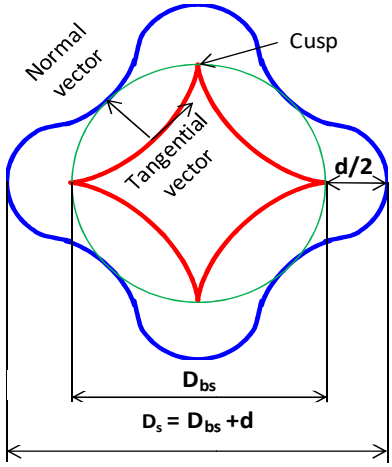

a: 4-lobe original and modified hypocycloid (4-lobe stator)

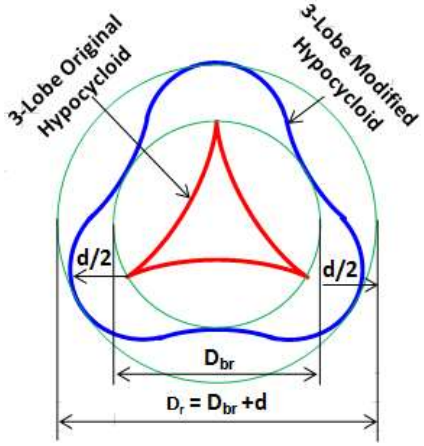

b: 3-lobe original and modified hypocycloid (3-lobe rotor)

Figure 2: Flowing cross-sectional area of a 3:4 (4-lobe) PDM

For the original hypocycloid, the relationship between the base diameters of stator and rotor can be expressed as (same generator circle diameter):

$$D_{br} = \frac{K-1}{K} D_{bs} \quad (12)$$

For the modified hypocycloid, the rotor diameter is base circle diameter plus semicircle diameter as shown in Fig. 2b. Combining Eq. (11) and Eq. (12) gives

$$D_r = D_{br} + d = \frac{K-1}{K} D_{bs} + d \quad (13)$$

Combining Eqs. (13) and (10) gives a relationship between stator and rotor diameters for a multi-lobe PDM as follows:

$$D_s = \frac{KD_r - d}{K-1} \quad (14a)$$

For a single lobe PDM, the relationship between stator and rotor diameters is given as,

$$D_s = 2D_r = 2d \quad (14b)$$

As shown in **Fig. 3**, the number of cavities (green shaded) of a K-lobe PDM is (K-1); e.g. for the 3:4 PDM, the number of cavities at any point along the pump is three. As the rotor of a K-lobe PDM turns 360/K degrees, the fluid in all cavities along single pitch length is displaced and moved completely to the cavities of the adjacent rotor pitch length as shown in **Fig. 4**. In other words, as the rotor movies from the very top of stator cusp to adjacent cusp, the fluid volume passes the motor is the product of flowing cross-sectional area, A_F, and rotor pitch length, P_r.

Therefore, the theoretical flow-rate of a PDM, which rotates at a rotational speed of N can be calculated as follows:

$$Q = A_F \times P_r \times K \times N \quad (15)$$

The relationship between rotor stator pitch lengths is given as:

$$\frac{P_s}{P_r} = \frac{K}{K-1} \quad (16)$$

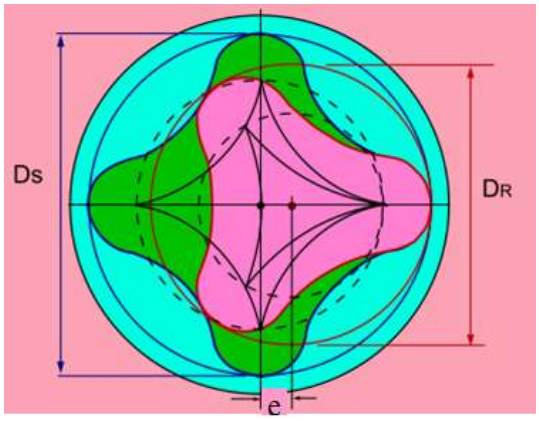

Figure 3: The cross-sectional view of 3:4 PDM (Robles, 2001)

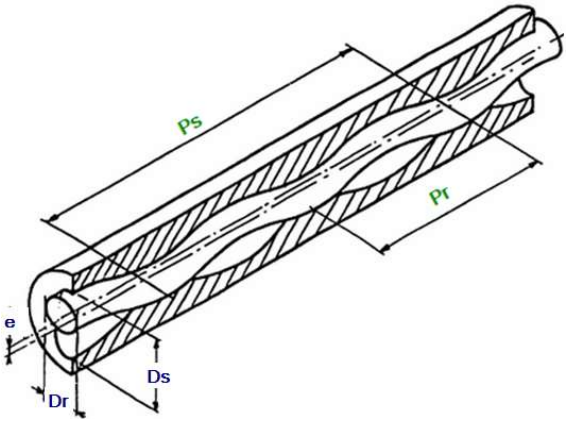

Figure 4: Rotor and stator pitch length of 1:2 PDM.

Combining Eqs. (4), (6) and (7) gives the theoretical flow-rate of any multi-lobe PDM as:

$$Q = [2\pi e^2(K-2) + 4de](K-1)P_s N \quad (17)$$

where P_r and P_s are rotor and stator pitch lengths, respectively; N is rotational speed in RPM. If the eccentricity, semicircle diameter, and pitch length are in the unit of inch, the rotational speed is in the unit of RPM. In gallon per minute, the flow rate is given as,

$$Q = 0.00433[2\pi e^2(K-2) + 4de](K-1)P_s N \quad (18)$$

The mechanical horsepower developed by the motor in SI and field units is defined as the product of its torque, T, by its angular velocity, $= \frac{2\pi N}{60}$, given respectively as,

$$HP_m(watts) = 2\pi N(RPM) \times T(m \times N) \quad (19)$$

$$HP_m(HP) = \frac{T(ft-lb\ ) \times N(RPM)}{5252} \quad (20)$$

The hydraulic horsepower for an incompressible fluid in SI and field units are, respectively, given as,

$$HP_h(watts) = 1.67 \times Q\left(\frac{L}{min}\right) \times \Delta P(bar) \quad (21)$$

$$HP_h(HP) = \frac{Q(GPM) \times \Delta P(psi)}{1714} \quad (22)$$

where Q is flow rate, and ΔP is differential pressure across motor. The overall motor efficiency is given as,

$$\eta = \frac{HP_m}{HP_h} = \frac{T \times N}{3.064 \times Q \times \Delta P} \quad (23)$$

In Eq. (23), torque, rotational speed, flow-rate, and pressure drop are in the unit of ft-lbf, RPM, GPM, and psi, respectively. Combining Eq. (18) and Eq. (23) gives the torque in ft-lbf as follows:

$$T = 0.01326[2\pi e^2(K-2) + 4de](K-1)P_s \Delta P \eta \quad (24)$$

where e, d and P_s are in the unit of inch, and ΔP is in the unit of psi. Eq. (24) indicates that torque of PDM is a function of

motor geometry (K, e, and d), pressure drop, and motor efficiency only. N.

Experimental Setup

An experimental facility was used to investigate the effect of operating conditions on the performance of a 1:2 and 2:3 PDM. The purpose of the experimental work was to validate the accuracy of Eq. (17), which is used to predict the performance of any multi-lobe PDMs. The schematic illustration of the experimental facility is shown in Fig. 5. The facility consists of the following main components: a 1:2 PDM or 2:3 PDM, a Coriolis mass flow-meter to measure flow-rates and fluid temperatures, two Rosemount pressure transmitters to measure the intake and the discharge pressure of the PDM, a control valve to control the back pressure, an 50-gallon liquid tank with an heater element and a propeller inside, an 50-gallon water tank. Summary of the geometrical parameters of the two motors is given in Table 1. Mineral oil with a density of 898 kg/m^3 was used to conduct all the tests. The rheological tests were conducted to obtain the relationship between viscosity, μ (cp), and temperature, Temp (^{o}F), of this mineral oil. The correlation is shown in Eq. (25).

$$\mu = 6813.5e^{(-0.034Temp)} \quad (25)$$

Table 1: Geometrical parameters of the two tested PDMs

Geometrical Parameters	Single lobe 1:2 PDM	Multi-lobe 2:3 PDM
Stator lobe number, K	2	3
Rotor diameter, D_r (mm)	14	18
Rotor pitch length, P_r (mm)	30	43
Eccentricity, e (mm)	3.5	3.7

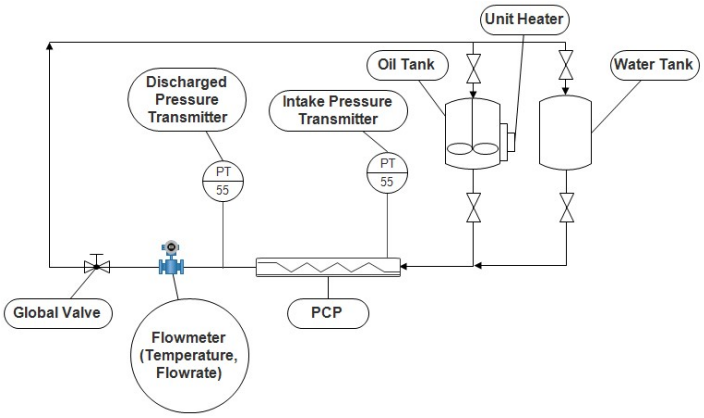

Figure 5: Schematic of the experimental facility

The test procedure is summarized as follows.

1. Set and maintain a desired rotational motor speed, e.g. 200 RPM.
2. Turn on the heater to a desired temperature to control the liquid viscosity.
3. Adjust the backpressure valve to obtain a desired value of the discharge pressure, e.g. 100 psi.
4. Record intake and discharge pressures across the motor, liquid flow rate, and fluid temperature downstream of the motor.

Modeling Results and Validation

Modeling Results

Let's consider a K-lobe PDM and define the maximum flow area (A_{max}) as the cross-sectional flowing area of the stator with K-lobe.

$$A_{max} = \frac{\pi D_S^2}{4} \quad (26)$$

where D_S is the stator diameter calculated using Eq. (10). In order to optimize the motor torque at different motor's lobe number, a dimensionless torque (T^*) is defined as the ratio between the torque (T), and the maximum torque (T_{max}) as,

$$T^* = \frac{T}{T_{max}} = \frac{0.01326A_F(K-1)P_s\Delta P\eta}{0.01326A_{max}(K-1)P_s\Delta P\eta} \quad (27)$$

Substituting Eq. (4) into Eq. (27) and simplifying gives,

$$T^* = \frac{T}{T_{max}} = \frac{A_F}{A_{max}} = \frac{2\pi e^2(K-2)+4de}{\frac{\pi D_S^2}{4}} \quad (28)$$

Substituting Eq. (10) into Eq. (28) and dividing the numerator and denominator of Eq. (28) by e^2 gives:

$$T^* = \frac{2\pi(K-2)+4\phi}{\frac{\pi}{4}(\phi+2K)^2} \quad (29)$$

where ϕ = d/e is dimensionless motor diameter. Differentiating Eq. (29) with respect to ϕ, and setting it equal to zero gives,

$$\frac{\partial T^*}{\partial \phi} = \frac{-16[\pi(K-2)+\phi-2K]}{\pi(2K+\phi)^3} = 0 \quad (30)$$

According to Eq. (30), the dimensionless torque (T*) reaches a maximum value when

$$\phi = 2K - \pi(K-2) \quad (31)$$

For a single-lobe PDM (K = 2), Eq. (31) gives ϕ = 2K = d/e = 4, indicating that to maximize motor torque, d has to be equal to 4e. When substituting K = 2 and d = 4e into Eq. (24), one may recognize that torque is proportional to the square root of d or e. Therefore, increasing the value of d or e will offer an exponential increase in torque for a single lobe PDM.

For multi-lobe PDM, Eq. (31) gives negative values of ϕ when

K > 5, which physically do not exist, thus $\phi = 0$ for K > 5. **Fig. 6** is a plot of dimensionless torque, T^*, versus dimensionless motor geometry, ϕ, for different stator's lobe number, K, indicating that maximum torque is at $\phi = 4$ for K = 2, i.e. single-lobe PDM. The combination of stator lobe number and dimensionless motor geometry to maximize torque is presented in **Fig. 7**. This result reveals that as stator lobe number increases, dimensionless motor geometry has to decrease to maximize torque. For stator lobe number is greater than five, the dimensionless number is zero to maximize torque. Note that, this analysis can be applied not only for torque, but also for motor flow rate and flowing cross-sectional area.

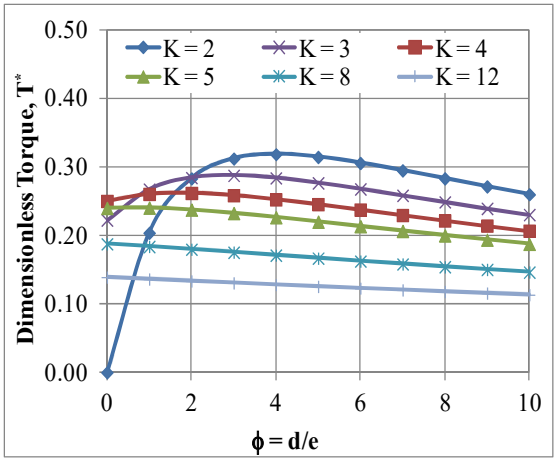

Figure 6: Optimization of motor torque at different dimensionless diameter

Rearranging Eq. (11), gives $d = D_r - 2e(K - 1)$, which when substituted into Eq. (17) and rearranged, gives:

$$Q = P_S N(K-1)\{[2\pi(K-2) - 8(K-1)]e^2 + 4D_r e\} \quad (32)$$

Differentiating Eq. (32) with respect to e and setting it equal to zero gives:

$$\frac{e}{D_r} = \frac{1}{[4(K-1) - \pi(K-2)]} \quad (33)$$

Eq. (33) indicates that for a specific multi-lobe PDM, and given rotor diameter, motor eccentricity can be designed to maximize flow rate (or torque). This relationship between e/D_r and K is presented in **Fig. 8**.

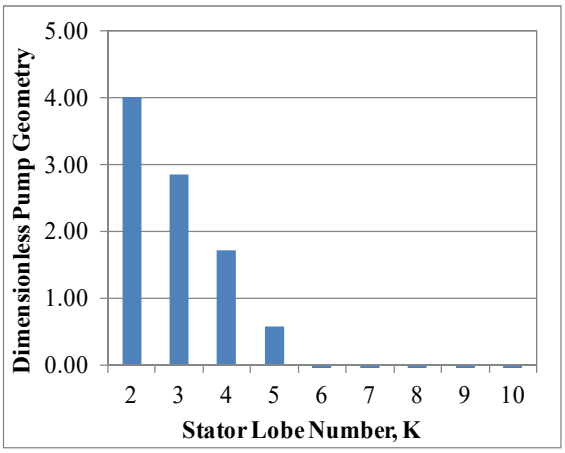

Figure 7: Relationship between K and dimensionless diameter at optimum torque

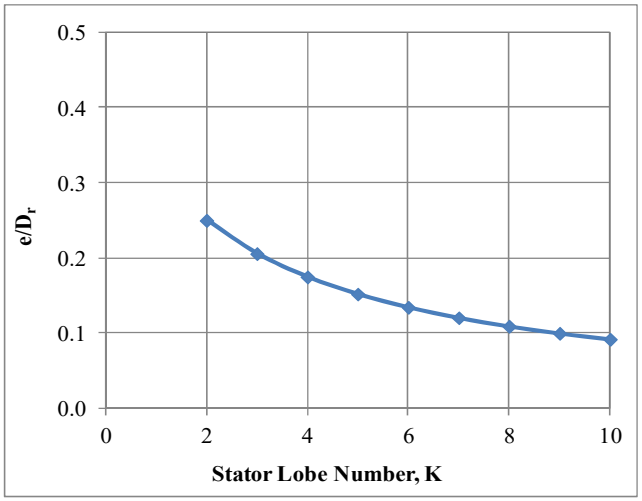

Figure 8: Optimization of motor eccentricity for maximum flow rate (or torque)

To study the effect of the number of motor lobes on flowing cross-sectional area and flow rate, let us consider a PDM with geometry given in **Table 2**.

Table 2: Simulated PDM Geometry

Stator diameter, D_s	6.98-cm	2 ¾-in.
Stator pitch length, P_s	106.68-cm	42-in.
Semicircle diameter, d	2.28-cm	0.35-in.
Eccentricity, e	Calculated using Eq. (10)	
Stator lobe number, K	Varied	

By changing the number of lobes, K, flowing cross-sectional area, motor eccentricity, and flow rate can be calculated using Eq. (4), Eq. (10), and Eq. (18), respectively. According to Eq. (10), for a given value of the semicircle diameter, as the stator lobe number increases, eccentricity decreases, thus dimensionless motor geometry increases. This relationship is shown in **Fig. 9**, which shows that a range of semicircle

diameter from d = 0.1 to 0.9 in., the maximum flowing cross-sectional area occurs at stator lobe number of either three or four. However, flow rate always increases as stator lobe number increases for a specific rotational speed as shown in **Fig. 10**. Although the flowing cross-sectional area decreases (with K ≥ 4) as the stator lobe number increases, the number of cavities within the rotor and stator is high, resulting in an increase in flow rate.

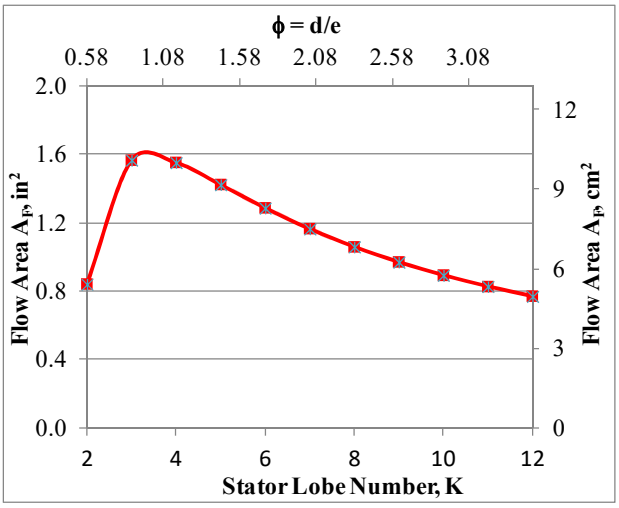

Figure 9: Effect of K on A_F
(D_s = 2 ¾-in., P_s = 42-in., d = 0.35-in.)

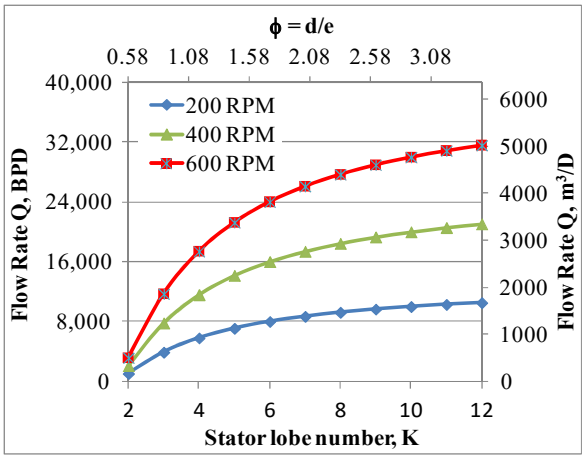

Figure 10: Effect of K on Q
(D_s = 2 ¾-in., P_s = 42-in., d = 0.35-in.)

To experimentally investigate the effect of motor lobe number on motor torque at different motor differential pressures, the data in Table 2 is used. Liquid is pumped through the motor with a constant flow rate of 1363 m^3/D (250 GPM), assuming motor efficiency of 0.75. Eq. (24) is used to calculate motor torque, and the results are illustrated in **Figs. 11** and **12**. Note that for a constant stator lobe number and constant differential pressure, torque is independent on the drill-bit speed as given by Eq. (24). However, as stator lobe number varies, drill-bit speed declines as the differential pressure ramps up, which is shown in the solid-smooth curve in Fig. 11. Furthermore, Fig. 11 presents the relationship between torque and motor differential pressure for four values of stator lobe number, namely 4 (3:4-lobe motor), 6 (5:6-lobe motor), 10 (9:10-lobe motor), and 12 (11:12-lobe motor). Generally, when increasing the stator lobe number, rotational speed decreases and torque increases for a constant value of differential pressure. As shown in Fig. 10, flow rate is proportional to the stator lobe number, leading to an increase in torque as shown in Eq. (24). However, this increase in torque reduces significantly when the stator lobe number is higher than ten as shown in Fig. 12. The percent increase in torque when the stator lobe number varies from 12 to 14 is approximately 3.6%. Therefore, it is recommended to design PDM with stator lobe number greater than 12.

In general, as long as mud pump can provide enough horsepower to PDM, it theoretically can handle high WOB. However, if the applied WOB is too high, differential pressure across power section and motor torque will be too high, causing a damage on the stator elastomer. Depending on the type of the elastomer, there is allowable differential pressure that can handled by the motor. If differential pressure is higher than the allowable, then stator will be damaged.

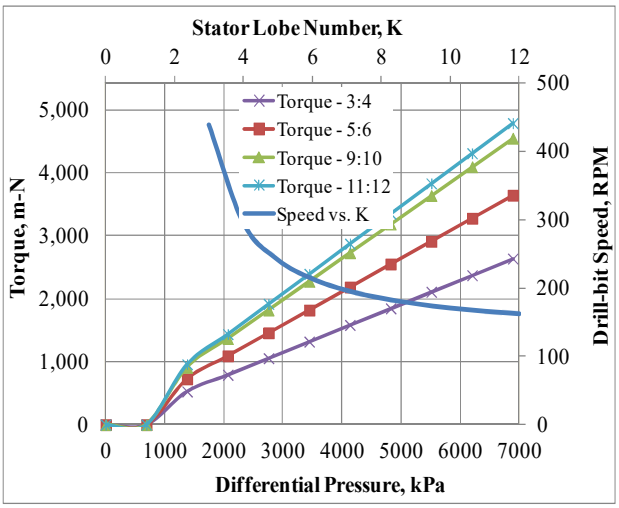

Figure 11: Effect of K on torque (Q = 250 GPM, η = 0.75,D_s = 2 ¾-in., P_s = 42-in., d = 0.35-in.)

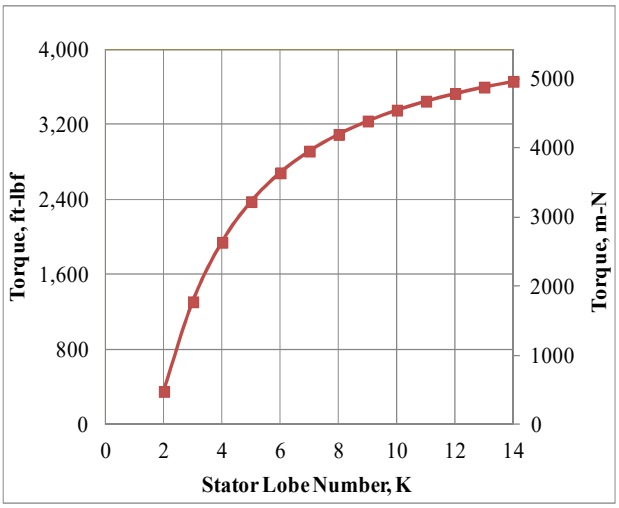

Figure 12: Optimizing torque based K values (Q = 250 GPM, η = 0.75, D_s = 2 ¾-in., P_s = 42-in., d = 0.35-in.)

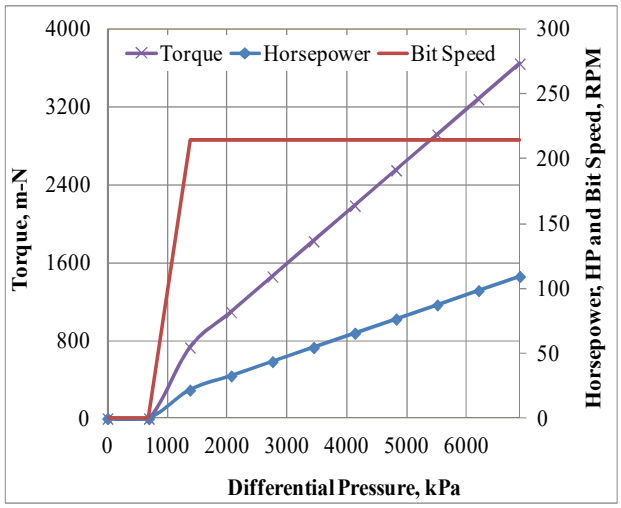

Figure 13: Performance of a PDM (Q = 250 GPM, η = 0.75, D_s = 2 ¾-in., P_s = 42-in., d = 0.35-in. K = 6)

Fig. 13 shows the theoretical prediction of a complete motor performance, which describes the relationship between torque, horsepower, and drill-bit speed vs. differential pressure across motor for the motor geometry presented in Table 2. In this particular simulation, the stator lobe number was kept constant as six (K = 6), as well as the liquid flow rate at 1363 m^3/D (250 GPM), with assumed motor efficiency of 0.75. The differential pressure to initiate motor rotation (to overcome the internal friction between the rotor and the stator) was assumed 689 kPa (100 psi). Using Eq. (10) and Eq. (18) to calculate motor eccentricity and theoretical drill-bit speed gave the values of 0.51-cm (0.2-in.) and 214 RPM, respectively. The results also revealed that as differential pressure varies from 689 to 6890 kPa (100 – 1000 psi), torque linearly increases from 0 to 3641 kPa (0 to 2685 psi), and horsepower linearly increases from 0 to 110 HP. However, if differential pressure is kept constant at 5512 kPa (800 psi), torque remains at 2913 kPa (2148 psi) regardless to the change in liquid flow rate as presented in **Fig. 14**. Eq. (24) indicates that for a specific motor geometry, when liquid flow rate varies, rotational speed also changes in such a way that torque remains the same for a constant differential pressure. In general, torque is independent on the rotational speed (or liquid flow rate) for a given motor, and operated at a constant differential pressure. Torque changes when motor geometry (rotor or stator diameter, eccentricity, and stator lobe number) or the differential pressure varies.

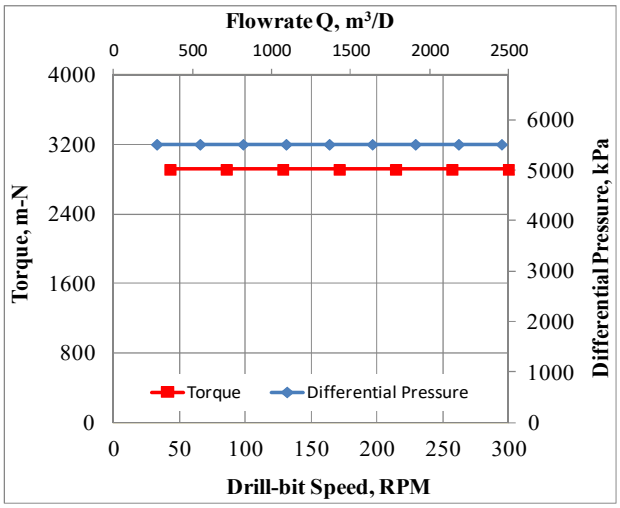

Figure 14: PDM Performance with variable Q and constant ΔP (η = 0.75, D_s = 2 ¾-in., P_s = 42-in., d = 0.35-in.)

Experimental Results and Model Validation

The performance of two motors, single 1:2-lobe PDM and multi 2:3-lobe PDM, were studied experimentally. The geometry of the two motors and the testing procedure is presented in the Experimental Setup section. The main purpose of the experimental work is to validate the accuracy of the developed Eq. (17). **Fig. 15** shows the comparison between experimental data and model prediction using Eq. (17) for the single 1:2-lobe PDM and the multi 2:3-lobe PDM at different rotational speeds. The tested fluid viscosity and the differential pressure were controlled at 380 cp and 100 psi, respectively. Under these conditions, the developed model predicts quite well the experimental data. At the rotational speed of 400 RPM, viscosity of 380 cp, and differential pressure of 100 psi, the comparison shows relative errors of about 13% and 3% for the 1:2-lobe PDM and 2:3-lobe PDM, respectively. The model predicts the performance of the 2:3-

lobe PDM better than that of the 1:2-lobe PDM. In general, the model will predict the performance of higher lobe PDMs better than that of lower lobe PDMs, because the higher lobe PDM has more sealing line within rotor and stator, hence reduces the internal slippage. The internal slippage is the difference between the theoretical and actual flow rates under a specific operating condition. In other words, the internal slippage is a countercurrent flow caused by insufficient displacement between the rotor and stator (Nguyen et al., 2016).

The impacts of fluid viscosity (110 – 440 cp) and differential pressure (100 – 300 psi) on the performance of the 2:3-lobe PDM at a rotational speed of 200 RPM is shown in **Fig. 16**. All the data and model prediction lie match well, with maximum relative error of about 6%. **Fig. 17** presents the effects of differential pressure across the motor and fluid viscosity on the performance of the 2:3-lobe PDM at three rotational speeds of 100, 300, and 600 RPM. The data revealed that when the fluid viscosity varies from 100 to 400 cp and the differential pressure is 200 psi or less, the internal slippage could be negligible. Under this testing condition, the maximum relative error recorded at rotational speed of 600 RPM and fluid viscosity of 120 cp is about 6%. In drilling operation, PDM is normally operated at a rotational speed of 400 RPM or less, and differential pressure of 6890 kPa (1000 psi) or less. From a practical point of view, one may draw a conservative conclusion that Eqs. (17) and (24) can be used to predict the actual performance of a multi-lobe PDM with the only care for the differential pressure. If the differential pressure of 300 psi or less, fluid viscosity of 100 cp or more, the model will predict actual performance of a multi-lobe PDM with a relative error of 6% or less.

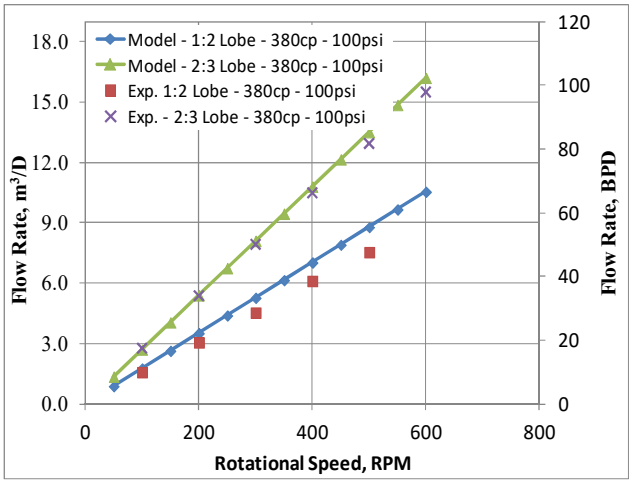

Figure 15: Model validation against experimental data for 1:2-lobe and 2:3-lobe PDMs

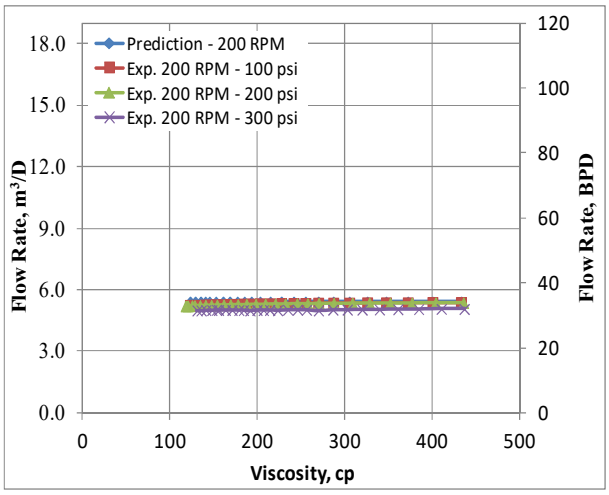

Figure 16: Model predicion comparison with experimental data for 2:3-lobe PDM with variable μ, ΔP at 200 RPM.

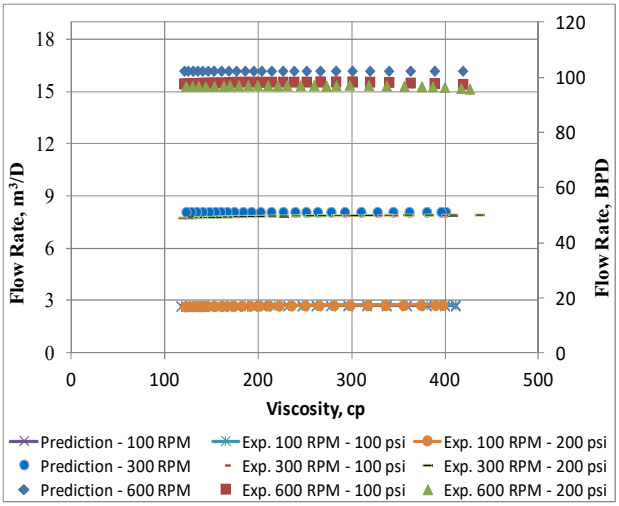

Figure 17: Model prediction comparison with experimental data for 2:3-lobe PDM with variable μ, ΔP and RPM.

Summary and Conclusions

This paper aims to develop a theoretical model to predict the performance of multi-lobe PDMs. An intensive sensitivity analysis was carried out to optimize the motor design to have a better understanding of the performance of PDMs. Several conclusions can be drawn from this study as follows:

- For stator lobe number greater than 5 (K > 5), torque is maximized if the dimensionless motor geometry approaches zero ($\phi = d/e = 0$). Practically, the semicircle diameter, d, must be greater than zero to minimize the internal slippage and hence motor eccentricity should be maximized to obtain the highest torque for K > 5.
- For a specific stator lobe number, Eq. (33) can be used to optimize the ratio between eccentricity and rotor diameter at which the flow rate or torque is maximum.

- For the stator lobe number greater four (K > 4), there will be a reduction in the flowing cross-sectional area as the stator lobe number increases. However, flow rate always increases when stator lobe number increases. This is because of the higher total volume of cavities within the rotor and the stator.
- Torque increases as lobe of the PDM increases. However, it is not recommend designing a PDM, which has stator lobe number greater than twelve. The increase in torque is 3.6% or less if the stator lobe number increases from 12 to 14 or higher.

If differential pressure across the motor is 300 psi or less, and the fluid viscosity is 100 cp or more, Eqs. (17) and (24) can be used to predict the actual multi-lobe PDM's performance with a relative error of less than 6%.

Acknowledgments

The authors thank all member companies of the Production and Drilling Research Project (PDRP) for their financial and technical support throughout this study. The authors also thank PDRP for allowing us to use the New Mexico Tech Pump Facility to collect all the data in this study.

Nomenclature

A = *Cross-sectional area, m^2 (in^2)*

A_K = *Cross-sectional area of a K-lobe hypocycloid, m^2 (in^2)*

A_F = *Cross-sectional flowing area of a positive displacement motor, m^2 (in^2)*

A^* = *Dimensionless area - ratio between the flow area (A_F) and the maximum area (A_{max}).*

d = *Diameter of the semicircle, m (in)*

D_b = *Diameter of the base circle, m (in)*

D_{br} = *Diameter of the rotor base circle, m (in)*

D_{bs} = *Diameter of the stator base circle, m (in)*

D_g = *Diameter of the generator circle, m (in)*

D_r = *Rotor diameter, m (in)*

D_s = *Stator diameter, m (in)*

e = *Motor eccentricity, m (in)*

HP_h = *Hydraulic horsepower, Watt (HP)*

HP_m = *Mechanical horsepower, Watt (HP)*

K = *Stator lobe number*

N = *Rotational speed or drill-bit speed, RPM*

P = *Pressure, Pa (psi)*

P_s = *Stator pitch length, m (in)*

P_r = *Rotor pitch length, m (in)*

Q = *Pump rate, m^3/D (gallon per minute)*

r_b = *Radius of the base circle, m (in)*

r_g = *Radius of the generator circle, m (in)*

T = *Motor torque, m-N (ft-lbf)*

T^* = *Dimensionless torque, unitless*

TVD = *True vertical depth, m (ft)*

Subscripts

b = *Base or bit*

br = *Base circle of the rotor*

bs = *Base circle of the stator*

f = *friction*

F = *Flow*

h = *Hydraulic*

g = *Generator*

K = *Stator lobe number*

m = *Mechanical or mud*

max = *Maximum*

p = *pump*

r = *rotor*

s = *stator*

wf = *Flowing bottom hole*

Superscripts

dp = *Drill-pipe*

ann = *Annuls*

* = *Dimensionless*

Greek letters

ϕ = *Dimensionless motor geometry – ratio between the semicircle diameter and the* eccentricity

η = *Motor efficiency*

References

Courgar Drilling Solutions, "Motor Operations Handbook" Version 5.0 – 2012.

Li, J., Tudor, R., Ginzburg, L., Robello, G., Xu, H., and Grigor, C.: "Evaluation and Prediction of the Performance of Positive Displacement Motor," SPE International Conference on Horizontal Well Technology, Alberta, Canada, November 1998.

Makohl, F., and Jurgens, R.: "Evolution and Differences of

Directional and High-Performance Downhole Motors," Presented at the IADC/SPE Drilling Conference held in Dallas, TX, February 1986 – IADC/SPE 14742.

Moineau, J.: "Pompe" Patent US No. 1 892 217, December 27, 1932.

Nguyen, T. C., Al-Safran, E., Saasen, A., and Nes, Olav-Magnar, "Modeling the Design and Performance of Progressing Cavity Pump Using 3-D Vector Approach," Journal of Petroleum Science and Engineering, 122 (2014) 180-186.

Nguyen, T. C., Tu, H., Al-Safran, E., Saasen, A., "Simulation of Single-phase Liquid Flow in Progressing Cavity Pump," Journal of Petroleum Science and Engineering, 147 (2016) 617-623.

Robles, J.: "Another Look to Multilobe Progressive Cavity Pump," SPE Progressing Cavity Pump Workshop, Puerto La Cruz, January 2001.

Samuel, R., Miska, S., Volk, L., "Analytical Study of the Performance of Positive Displacement Motor (PDM): Modeling for Incompressible Fluid," Presented at the Fifth Latin American and Caribbean Petroleum Conference and Exhibition held in Rio de Janeiro, Brazil, September 1997 – SPE 39026.

Samuel, R., Miska, S., "Performance of Positive Displacement Motor (PDM) Operating On Air," Journal of Energy Resources Technology, Vol. 125, (119-125), June 2003.

Roberts, B., and Mohr, C., "Down-hole Motors for Improved Drilling," Journal of Petroleum Technology (JPT), (1484 - 1490), 3343, Dec. 1972